Superdeformation and α-cluster structure in ^{35}Cl

Abhijit Bisoi,[1] M. Saha Sarkar,[1,*] S. Sarkar,[2] S. Ray,[1] M. Roy Basu,[3] Debasmita Kanjilal,[1] Somnath Nag,[4] K. Selvakumar,[4] A. Goswami,[1] N. Madhavan,[5] S. Muralithar,[5] and R. K. Bhowmik[5]

[1]*Saha Institute of Nuclear Physics, Bidhannagar, Kolkata 700064, India*
[2]*Bengal Engineering and Science University, Shibpur, Howrah 711103, India*
[3]*University of Calcutta, Kolkata 700009, India*
[4]*Indian Institute of Technology, Kharagpur 721302, India*
[5]*Inter-University Accelerator Centre, New Delhi 110067, India*

(Received 16 January 2013; revised manuscript received 25 April 2013; published 3 September 2013)

A superdeformed (SD) band has been identified in a non-α-conjugate nucleus ^{35}Cl. It crosses the negative-parity ground band above $11/2^-$ and becomes the yrast at $15/2^-$. Lifetimes of all relevant states have been measured to follow the evolution of collectivity. Enhanced $B(E2)$, $B(E1)$ values as well as energetics provide evidence for superdeformation and existence of parity doublet cluster structure in an odd-A nucleus in the $A \simeq 40$ region. Large-scale shell-model calculations assign $(sd)^{16}(pf)^3$ as the origin of these states. Calculated spectroscopic factors correlate the SD states in ^{35}Cl to those in ^{36}Ar.

DOI: 10.1103/PhysRevC.88.034303 PACS number(s): 21.10.Re, 21.10.Tg, 21.60.Cs, 27.30.+t

I. INTRODUCTION

The superdeformed (SD) bands observed in the even-even nuclei in the upper sd shell have provided favorable conditions to describe the collective rotation microscopically involving the cross-shell correlations [1,2]. Complementary descriptions in terms of particle-hole excitations in the shell model [2,3] and α-clustering configurations within various cluster models [4–6] have been utilized to interpret the data. To our knowledge no such band has been previously observed in non-α-conjugate odd-A, $N \neq Z$ isotopes in this region [7]. If a nucleus clusters into fragments of different charge-to-mass ratios, the center of mass does not coincide with its center of charge. As a result a sizable static $E1$ moment may arise in the intrinsic frame [8], resulting in several distinctive features in the spectra. Two adjacent opposite-parity deformed $\Delta I = 2$ bands connected by strong $E2$ intraband transitions in turn are connected by strong $E1$ interband transitions [8], forming an apparent $\Delta I = 1$ rotational band with alternating parity states. Since the early seventies [9–11], a number of similar α-cluster bands have been studied extensively. In the spectrum of ^{19}F, cluster-model calculations have shown that coupling of a proton hole in the p shell coupled with four nucleons in the sd shell (a proton hole coupled to ^{20}Ne) gives rise to α-cluster bands. The lowest $\alpha + ^{15}N$ parity partner bands built on the $K^\pi = 1/2^+$ ground-state band, the lowest-lying $K^\pi = 1/2^-$ at 110 keV, and some other bands lying above 5 MeV have been observed. So far no similar clusterings have been observed in odd-A nuclei in the $A \simeq 40$ region, where evidence of clustering has manifested in even-even nuclei through superdeformation.

According to Ikeda [12], in the spectra of light nuclei, clusterlike configurations would appear near the threshold energy needed for breakup into proper subnuclei. For the nucleus of our interest, ^{35}Cl, the threshold energy [13] to appear as a composite of ^{32}S and a triton (t) ($^{32}\mathrm{S} + t$) is around 18 MeV. On the other hand, threshold for the decay of the composite system ^{35}Cl into ($^{31}\mathrm{P} + \alpha$) clusters is around 6.5 MeV. The SD rotational band observed in ^{36}Ar has been shown to have a cluster structure, so one may also expect to find deformed cluster bands in the excitation spectra of ^{35}Cl generated by coupling a proton hole to SD states in ^{36}Ar.

In this article, we report the observation of a superdeformed band in the odd-A ^{35}Cl isotope. The reduced transition probabilities for all relevant transitions depopulating the states of the yrast negative-parity band and related positive-parity ones have been determined from lifetimes measured in the present experiment. Extracted $B(E2)$s and $B(E1)$s provide important information to probe the remnant of clustering in ^{35}Cl. Large-basis shell-model (LBSM) calculations have been done to understand the evolution of collectivity along this band. The predicted [4] negative-parity partner band of the SD band in ^{36}Ar has also been reproduced within LBSM calculations. Spectroscopic factors have been used to correlate the SD states in ^{35}Cl to the cluster states in ^{36}Ar to establish the persistence of α-clustering features.

II. EXPERIMENTAL DETAILS

High spin states of ^{35}Cl have been populated through $^{12}\mathrm{C}(^{28}\mathrm{Si},\alpha p)^{35}\mathrm{Cl}$ reaction in the inverse kinematics with an 110-MeV ^{28}Si beam at the Inter-University Accelerator Center (IUAC), New Delhi. The target was ^{12}C (50 $\mu g/\mathrm{cm}^2$) evaporated on 18 mg/cm^2 Au backing. The γ-γ coincidence measurement has been done using the multidetector array of thirteen Compton suppressed clover detectors (Indian National Gamma Array: INGA setup). The relevant details of the experimental setup have been discussed in Ref. [14]. The detectors were placed at 148° (4), 123° (2), 90° (4), 57° (2) and 32° (1). The experimental data have been sorted into angle-dependent symmetric (90° vs 90°) and asymmetric γ-γ matrices to get the information about the γ intensities, Directional Correlation (DCO) ratios, and level lifetimes of this band.

*maitrayee.sahasarkar@saha.ac.in

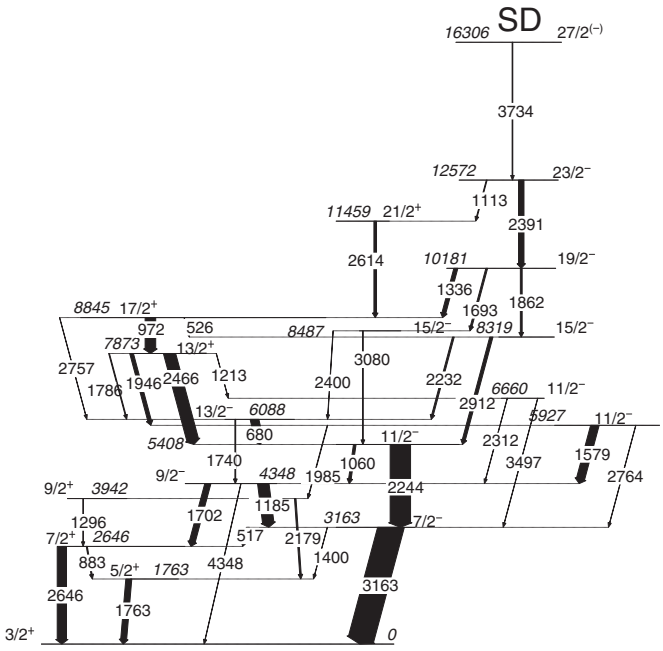

FIG. 1. Partial level scheme of ^{35}Cl.

III. DATA ANALYSIS AND RESULTS

In our earlier work [15], we reported a few totally shifted γ rays in the spectra emitted from states having lifetimes shorter than the characteristic stopping time ($\simeq 10^{-13}$ s) of ^{35}Cl recoils in gold (Au) backing. Analysis of the present data confirmed [16] that four of them (2912, 1862, 2391, and 3734 keV) belong to the same sequence (marked as SD in Fig. 1), which is connected to the other states in ^{35}Cl through 1113, 1336, 2232, and 1693 keV transitions (Fig. 1). The lowest state of this sequence, 5408 keV ($11/2^-$), is already known to be connected to the 3163-keV ($7/2^-$) state through a strong 2244-keV transition [11]. This sequence from 3163-keV ($7/2^-$) state to the 16306-keV ($27/2^-$) state has been established as the yrast negative-parity band. The three topmost transitions in the band show nearly perfect rotational behavior by the almost linear increase in angular momentum with γ-ray energy (rotational frequency) (Fig. 2). The plot shows a sharp break between $15/2^-$ to $19/2^-$, indicating a crossing between two weakly interacting bands of different configurations. The kinematic moment of inertia (KMOI) for the top three transitions in yrast band in ^{35}Cl scaled by the mass factor compares very well with those for SD bands in ^{36}Ar and ^{40}Ca. The average KMOI, $\simeq 8\ \hbar^2$/MeV, also compares well with the candidate SD band in ^{28}Si ($\simeq 6\ \hbar^2$/MeV) [6]. More dramatically, the inset of Fig. 2 shows that energies of alternating parity states $15/2^-$, $17/2^+$, $19/2^-$, $21/2^+$, $23/2^-$, and $27/2^-$ follow a linear relation to the $I(I+1)$ values exhibiting an apparent rotational band structure, which characterises nuclear molecular structure [8].

Line shapes of all γ rays in the yrast sequence (except the 2244-keV γ), along with the 2614-keV γ ray connecting the $21/2^+$ state to $17/2^+$, have been analyzed to determine the lifetimes of the corresponding states. Due to the large recoil velocity in inverse kinematics and high energies of the relevant

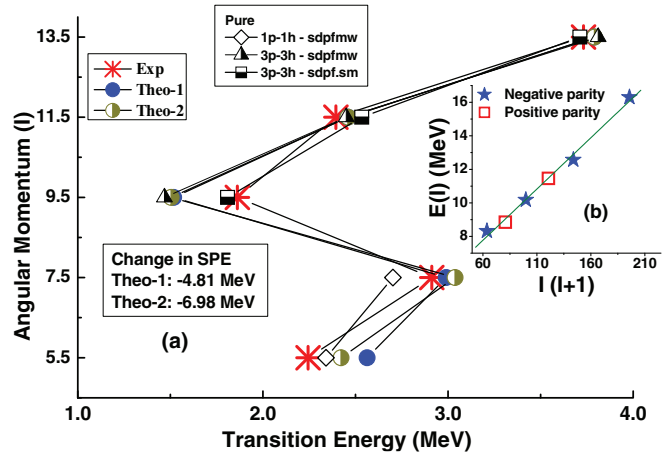

FIG. 2. (Color online) (a) Comparison of experimental and theoretical back-bending plots for the yrast negative-parity band in ^{35}Cl. The figure shows the results of calculations with fixed $n\hbar\omega$ and mixed $n\hbar\omega$ truncations, viz., Theo1: $[(1d_{5/2})^{12}(2s_{1/2}1d_{3/2})^6(pf)^1 \oplus (1d_{5/2})^{12}(2s_{1/2}1d_{3/2})^4(pf)^3]$; Theo2: $[(sd)^{18}(pf)^1 \oplus (1d_{5/2})^{12}(2s_{1/2}1d_{3/2})^4(pf)^3]$. The amount of depression of the single-particle energies (SPEs) of pf orbitals in each truncation scheme is also mentioned. (b) The energies ($E(I)$) of $15/2^-$, $17/2^+$, $19/2^-$, $21/2^+$, $23/2^-$, and $27/2^-$ states are plotted as function of $I(I+1)$.

γs, special care has been taken to choose the gating transitions such that the slow feeding components are eliminated. Gating from the top could not be done due to poor statistics. However, while choosing a suitable gating transition from below, special care has been taken to eliminate the contribution of strong γ peaks close to the peaks of interest. The spectra at mean angles of 148° and 90° relative to the beam axis were simultaneously fitted (Fig. 3) using a modified version of the LINESHAPE [17,18] code which included corrections for the broad initial recoil momentum distribution produced by the α-particle evaporation. The initial momentum distribution of ^{35}Cl recoils has been obtained from statistical model

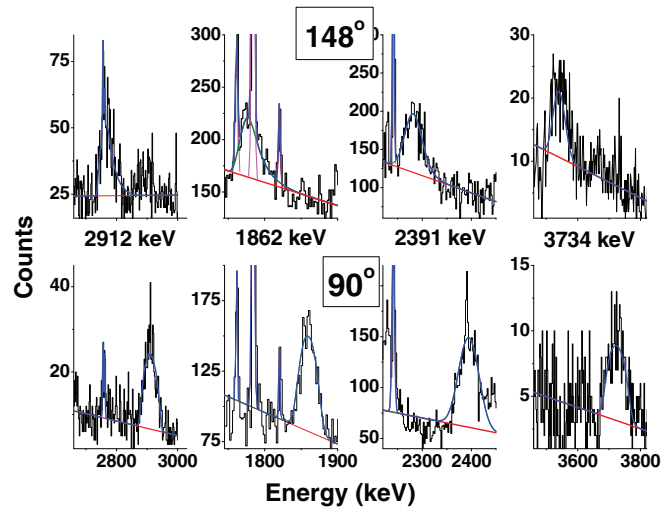

FIG. 3. (Color online) The experimental and calculated Doppler-shifted line shapes for different transitions. The transition energies and angles are indicated in the figure.

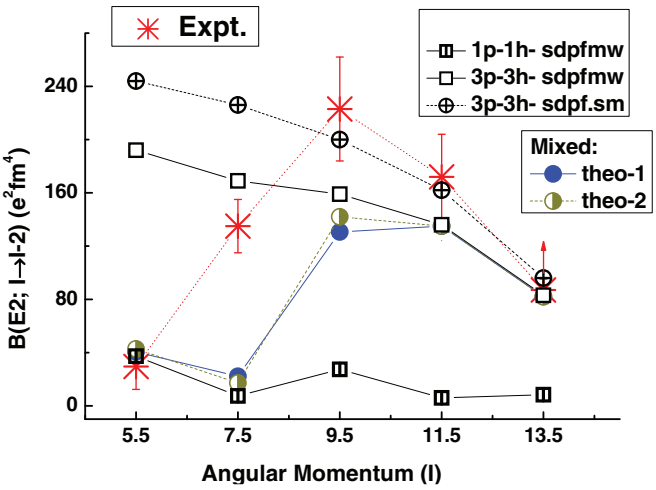

FIG. 4. (Color online) Experimental $B(E2; I_i \rightarrow I_f)$ values for the yrast band in ^{35}Cl compared with the results of shell-model calculations.

code PACE4 [19]. Line shapes of four γ transitions (3734, 2391, 1862, and 2912 keV) were fitted simultaneously as members of a single band. The rotational cascade side feeding has been considered, assuming 100% side feeding into the top of the band. During each line-shape simulation, the background parameters, intensities of the contaminant peaks, and side-feeding quadrupole moments were allowed to vary, and the best fit set was obtained by using the χ^2 minimization. The line shape of the 1336-keV transition has also been fitted to get an independent estimate of the lifetime of the 10 181-keV level. Using the relevant branching ratios [11], experimental $B(E2)$s were determined from these lifetimes (Fig. 4, Table I). The collectivity in this negative-parity band evolves from single-particle excitations ($B(E2) \simeq 5$ W.u.) at lower spins, to a set of highly deformed SD states ($B(E2)$ $\simeq$ 20–33 W.u.) in between, finally terminating at a state at $27/2^-$ with moderate deformation ($B(E2) \simeq 13$ W.u.). The γ transition (2614 keV) connecting the positive-parity states also has comparable $B(E2)$ ($\simeq$16 W.u.) The decay-out transitions (1336 and 1113 keV) have relatively large $B(E1)$ values, viz., 2.9 and 2.6 $\times 10^{-3}$ W.u., respectively. In ^{36}Ar and ^{40}Ca, with 4p-4h and 8p-8h excitations in the pf $(N = 3)$ shell, the deformations (β_2) in the SD bands were 0.45 [2] and $\simeq$ 0.59 [1], respectively. In ^{35}Cl, 3p-3h excitations (discussed below) give rise to SD structure with comparable KMOI but relatively smaller deformation ($\simeq$0.37) (Table I) similar to the observation in heavier nuclei where the occupation numbers of high-N orbitals have been found to characterize SD bands.

TABLE I. Experimental level lifetimes, experimental and theoretical (Theo2) reduced transition probabilities ($B(L)$) for different transitions, corresponding transition quadrupole moments, Q_t (eb), together with quadrupole deformation (β_2) and X (major to minor axis ratio of an ellipsoid) deduced [20] from Q_ts are tabulated. The units of $B(E1)$, $B(E2)$, and $B(M1)$ are $10^{-3}\, e^2$ fm^2, e^2 fm^4, and $10^{-2}\, \mu_N^2$, respectively. The effective charges are $e_p = 1.5e$, $e_n = 0.5e$. For $B(M1)$ calculations, free single-particle g factors have been used.

I_i^π	τ_{mean} (fs)	E_γ (keV)	$B(L)$ Exp.	$B(L)$ Theo2	Q_t (eb)	β_2	X
$11/2^-$	400(100) [21]	2244 ($E2$)	29(8)	43	0.31(4)	0.15	1.16
$15/2^-$	18(1)	2912 ($E2$)	135(10)	17	0.65(2)	0.30	1.32
		2232 ($M1$)	<10	1.3			
$19/2^-$	61(4)	1862 ($E2$)	224(31)	142	0.82(6)	0.37	1.41
	61(7)	1336 ($E1$)	1.98(2)	1.03			
		1693 ($E2$)	148(41)	15			
$23/2^-$	48(6)	2391 ($E2$)	172(22)	135	0.71(5)	0.32	1.35
		1113 ($E1$)	1.8(2)	1.22			
$27/2^-$	<13	3734 ($E2$)	>87	82	>0.5	0.24	1.25
$21/2^+$	62(3)	2614 ($E2$)	108(5)	67	0.56(2)	0.27	1.28

IV. THEORETICAL ANALYSIS AND DISCUSSION

Large-basis shell-model (LBSM) calculations have been done using the SDPFMW Hamiltonian [22] (as referred to within the OXBASH code package [23]). The SDPFSM [1–3] Hamiltonian suitable for fixed n$\hbar\omega$ [3] excitation has also been used. The valence space consists of full sd-pf orbitals for both protons and neutrons above the ^{16}O inert core (see Ref. [15] for details). The negative- (positive-) parity spectra have been calculated with pure $\hbar\omega = 1$ (0) and 3 (2) excitations (Fig. 2). The experimental γ energies [$E_\gamma = E(I) - E(I-2)$] and corresponding $B(E2)$s for lowest state ($I = 11/2^-$) and the upper three states ($I = 19/2^-$ to $27/2^-$) agree reasonably well with the calculated values with 1p-1h and 3p-3h excitations, respectively. The results with SDPFSM exhibit better agreement with the experimental data for spins $19/2^-$ to $27/2^-$ (Figs. 2 and 4). However, for $I = 15/2^-$, although the γ energy agrees well with 1p-1h results, the experimental $B(E2)$ matches better to the theoretical $B(E2)$ values from 3p-3h calculations (Fig. 4). The reduction in experimental $B(E2)$ at $27/2^-$ is reproduced well by theory. This decrease indicates band termination at $27/2^-$, consistent with a proton hole coupled to the terminating spin (16^+) in the superdeformed band in ^{36}Ar nucleus [2,3].

Configuration mixing between 1p-1h, 3p-3h configurations has been included for further improvement of the results. The set Theo1 has inert $1d_{5/2}$ in 1p-1h excitation, whereas in Theo2, this orbital was active (Fig. 2). Inclusion of 5p-5h configurations has been found to be insignificant. It has been shown earlier that to reproduce the experimental data, the sd-pf shell gap has to be decreased depending upon the particular truncation scheme involved [15,24]. In the experimental spectra (Fig. 1), two close-lying $15/2^-$ states (energy difference is $\simeq$169 keV) are seen. The single-particle energies (SPE) of the pf orbitals have been shifted downwards to reproduce the splitting between the two lowest $15/2^-$ states. Results from mixed calculations show improvement in reproducing the γ energy of $15/2^-$ state (Fig. 2) deteriorating the agreement for $B(E2; 15/2^- \rightarrow 11/2^-)$ value. The reduced transition probabilities of decay-out $E1$ transitions (1336, 1113 keV) are reproduced well (Table I). Shell-model calculations reproduce the transition energy and $B(E2)$ of the 2614-keV transition reasonably well. The highest limit of experimental $B(M1)$ for the 2232-keV transition is larger than the predicted value. However, the calculated values of $B(E2;$

TABLE II. Comparison between wave functions of different states obtained from empirical fit and theoretical calculations. The 3p-3h components can be determined from normalization condition.

E_x	I_i	E_γ^{decay}	Wave function (1p-1h)		
			Emp.	Theo1	Theo2
10181	$19/2_1$	1862	0		0
8319	$15/2_1$	2912	9	13	8
5408	$11/2_1$	2244	16	68	76
3163	$7/2_1$	3163	94	75	80

$19/2_1^- \rightarrow 15/2_2^-$) (1693 keV) and $B(E2; 15/2_1^- \rightarrow 11/2_1^-)$ (2912 keV) both are severely underpredicted (Table I), indicating inadequacy of the configuration mixed calculations. In ^{36}Ar and ^{40}Ca also [2,3], the calculations failed to reproduce the transition probabilities for the states where different configurations interact to their maximum.

A simple phenomenological approach [25] using two-level mixing between pure 3p-3h and 1p-1h states have been used to determine the extent of configuration mixing existing in the states near the band crossing. In this calculation the $19/2^-$ state has been assumed to be a 3p-3h state (100%) with no mixing from 1p-1h (0%). Utilising the transition matrix elements from pure 1p-1h and 3p-3h LBSM calculations, the experimentally observed $B(E2; I \rightarrow I-2)$ values for the transitions with $I < 19/2^-$ have been reproduced considering the mixing coefficients of two-component wave function for each state as variables (Table II). The shell-model predictions deviate from the phenomenologically determined wave-function structure only for the $11/2^-$ state. It is evident that this deviation leads to the large difference between the experimental and predicted (Theo1 and Theo2) $B(E2)$ for the $15/2^- \rightarrow 11/2^-$ transition.

The SD band in ^{36}Ar has been shown to originate from the band crossing of $[^{32}\text{S}(I^\pi = 0^+ - 8^+) + \alpha]$ cluster bands [4]. The existence of a negative-parity partner band of the SD band is also predicted [4]. Even in the shell-model picture, a negative-parity partner of the SD band in ^{36}Ar has been obtained in terms of 3p-3h excitation $[(sd)^{17}(pf)^3]$ in the pf shell. So far, it has not been verified experimentally. The parentage of the negative-parity SD states in ^{35}Cl in terms of a proton hole coupled to the α-cluster SD states in ^{36}Ar core, have been obtained from calculated spectroscopic factors (Theo1) (Fig. 5). The $15/2^-$ to $27/2^-$ states in ^{35}Cl are generated primarily from the cluster SD states, 10^+ to 16^+, whereas the $17/2^+$ and $21/2^+$ arise predominantly from the 11^- and 13^- states in the negative-parity partner band in ^{36}Ar. The observed $17/2^+$ and $21/2^+$ states in ^{35}Cl therefore provide indirect experimental evidence in favor of the existence of a negative-parity partner band of the SD band in ^{36}Ar as predicted in Ref. [4] and the present work.

Using the weak coupling model [10], the interaction energy (of SD states in $^{36}\text{Ar} + \pi 1f_{7/2}$ hole) which gives rise to the SD states in ^{35}Cl has been calculated. The $\text{E}(\pi 1f_{7/2})_{\text{hole}}$ has been estimated from the excitation energy of the $7/2^-$ state in ^{35}Cl at 3163 keV. For example, $V_{\text{int}}(15/2^-$ in $^{35}\text{Cl}) = [\{BE$ (10^+ SD in ^{36}Ar) $- E$(hole in $1f_{7/2}$)$\}$ $- BE$ ($15/2^-$ SD in ^{35}Cl)].

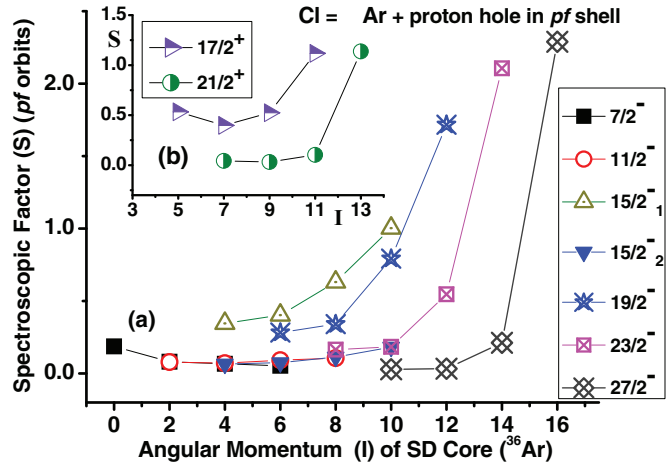

FIG. 5. (Color online) Calculated spectroscopic factors (Theo1) for the (a) negative-parity SD states in ^{35}Cl and (b) positive-parity partner states to estimate the contribution of the positive-parity even-spin SD states and their negative-parity odd-spin partners of the core nucleus, ^{36}Ar.

These estimations show that to generate $15/2^-$ to $27/2^-$ SD states in ^{35}Cl, by coupling a proton hole with 10^+ to 16^+ SD states in ^{36}Ar, the interaction energies [13] are 915, 175, −382, and −714 keV, respectively. These are small compared to a few-MeV average particle-particle interaction, and in two of the cases are repulsive, which is favorable for cluster structure formation. The unequal masses of the underlying clusters give rise to dipole degree of freedom, leading to the formation of an apparent rotational band containing alternating parity sequence (Fig. 2) connected by strong $E1$ transitions. These $E1$ transitions are stronger than 2×10^{-3} W.u., indicating that the corresponding positive-parity states are doublet partners [8].

V. SUMMARY

To summarize, a superdeformed rotational band with average transition quadrupole moment $Q_t \simeq 0.75$ eb and kinematic moments of inertia $\simeq 8\,\hbar^2$/MeV has been identified for in odd ^{35}Cl which terminates at $27/2^-$. The energies of alternating parity states, $15/2^-$, $17/2^+$, $19/2^-$, $21/2^+$, $23/2^-$, and $27/2^-$ connected by strong $B(E1)$s ($>2 \times 10^{-3}$ W.u.) and strong cross-over $E2$ transitions, follow a linear relation to the $I(I+1)$ values, providing strong evidence in favor of cluster structure of these states. Results of LBSM calculations have shown that the SD band has been generated by 3p-3h excitations $[(sd)^{16}(pf)^3$configuration]. A simple two -level mixing calculation has been done to extract the wave-function structure of these mixed states from the experimental $B(E2)$ values. Weak coupling estimation in terms of ^{36}Ar and a proton hole clearly identifies the origin of each SD state. The spectroscopic factors are calculated to estimate parentage of these SD states and their partners in terms of a proton hole coupled to the α cluster SD states in ^{36}Ar core. The observed $17/2^+$ and $21/2^+$ states in ^{35}Cl therefore provide indirect experimental evidence in favor of the existence of a negative-parity partner band of the SD band in ^{36}Ar as predicted in Ref. [4] and the present work.

ACKNOWLEDGMENTS

The authors acknowledge the help from all other INGA collaborators and the Pelletron staff of IUAC for their sincere help and cooperation. Special thanks are due to Pradipta Das for his technical help for target preparation. Discussions with P. Banerjee and A. K. Singh during analysis of the DSAM data are gratefully acknowledged. One of the authors (A.B.) has been financially supported by the Council of Scientific and Industrial Research (CSIR), India, under Contract No. 09/489(0068)/2009-EMR-1.

[1] E. Ideguchi *et al.*, Phys. Rev. Lett. **87**, 222501 (2001); C. J. Chiara *et al.*, Phys. Rev. C **67**, 041303(R) (2003).
[2] C. E. Svensson *et al.*, Phys. Rev. Lett. **85**, 2693 (2000); Phys. Rev. C **63**, 061301(R) (2001).
[3] E. Caurier, F. Nowacki, and A. Poves, Phys. Rev. Lett. **95**, 042502 (2005); E. Caurier, J. Menèndez, F. Nowacki, and A. Poves, Phys. Rev. C **75**, 054317 (2007).
[4] T. Sakuda and S. Ohkubo, Nucl. Phys. A **744**, 77 (2004).
[5] J. Cseh, A. Algora, J. Darai, and P. O. Hess, Phys. Rev. C **70**, 034311 (2004); Y. Taniguchi, M. Kimura, Y. Kanada-En'yo, and H. Horiuchi, *ibid.* **76**, 044317 (2007).
[6] D. G. Jenkins *et al.*, Phys. Rev. C **86**, 064308 (2012); J. Darai, J. Cseh, and D. G. Jenkins, *ibid.* **86**, 064309 (2012).
[7] Eric D. Johnson, Ph.D. thesis, Florida State University, 2008 (unpublished), and references therein.
[8] Y. Alhassid, M. Gai, and G. F. Bertsch, Phys. Rev. Lett. **49**, 1482 (1982); M. Gai, M. Ruscev, D. A. Bromley, and J. W. Olness, Phys. Rev. C **43**, 2127 (1991); S. Courtin, A. Goasduff, and F. Haas, arXiv:1303.4252v1 [nucl-ex], and references therein.
[9] B. Buck and A. A. Pilt, Nucl. Phys. A **280**, 133 (1977); M. Kimura and N. Furutachi, Phys. Rev. C **83**, 044304 (2011), and references therein.
[10] A. Arima and I. Hamamoto, Annu. Rev. Nucl. Sci. **21**, 55 (1971).
[11] http://www.nndc.bnl.gov
[12] K. Ikeda, N. Takigawa, and H. Horiuchi, Prog. Theo. Phys. Suppl. extra number: **464** (1968).
[13] G. Audi and W. Meng (private communication); G. Audi *et al.*, Chin. Phys. C **36**, 1287 (2012).
[14] S. Muralithar *et al.*, Nucl. Instrum. Methods A **622**, 281 (2010).
[15] R. Kshetri *et al.*, Nucl. Phys. A **781**, 277 (2007); A. Bisoi *et al.*, Proc. DAE-BRNS Symp. Nucl. Phys. (India) **55**, 4 (2010).
[16] F. Della Vedova *et al.*, Phys. Rev. C **75**, 034317 (2007); LNL Annual Report 2004, http://www.lnl.infn.it/~annrep/read_ar/2004/contrib_2004/pdfs/A130.pdf.
[17] J. C. Wells and N. R. Johnson, Oak Ridge National Laboratory (ORNL) Physics Division Progress Report ORNL-6689, 1991, p. 44.
[18] R. K. Bhowmik (private communication).
[19] A. Gavron, Phys. Rev. C **21**, 230 (1980).
[20] http://www.physics.mcmaster.ca/~balraj/sdbook/.
[21] P. R. G. Lornie *et al.*, J. Phys. A **7**, 1977 (1974).
[22] E. K. Warburton, J. A. Becker, and B. A. Brown, Phys. Rev. C **41**, 1147 (1990).
[23] B. A. Brown *et al.*, MSU-NSCL Report No. 1289, 2004 (unpublished).
[24] I. Ray *et al.*, Phys. Rev. C **76**, 034315 (2007); M. Saha Sarkar, Proc. DAE-BRNS Symp. Nucl. Phys. (India) **55**, I19 (2010); http://www.sympnp.org/proceedings/index.php
[25] H. T. Fortune, Phys. Rev. C **86**, 024305 (2012).